Journal of Fish Biology (1999) **54**, 1275–1286
Article No. jfbi.1999.0959, available online at http://www.idealibrary.com on IDEAL®

Blood flow distribution and tissue allometry in channel catfish

I. R. SCHULTZ*¶, M. G. BARRON†, M. C. NEWMAN‡ AND A. M. VICK§

**Battelle PNNL, Molecular Bioscience Division, P.O. Box 999-P7-56, Richland, WA 99352, U.S.A.; †Hagler Bailly, Inc., P.O. Box Drawer O, Boulder, CO 80306-1906, U.S.A.; ‡Department of Environmental Sciences, The College of William and Mary, Virginia Institute of Marine Science, School of Marine Science, Gloucester Point, VA 23062-1346, U.S.A. and §College of Pharmacy Ohio State University, 500 West 12th, Columbus, OH 43210, U.S.A.*

(*Received 18 August 1998, Accepted 23 February 1999*)

Blood flow (as percentage of cardiac output) in fasted channel catfish acclimated to 21° C was directed primarily to white muscle (72%) followed by head kidney (5·7%), red muscle (5·5%), trunk kidney (3·1%), liver (2·2%), swim bladder (1·4%) and skin (1·1%). The stomach, intestines, pyloric caeca, gonads, brain, abdominal fat and spleen contained <0·5% of blood flow. There was considerable interfish variation among blood flow distribution to visceral organs with substantial spatial heterogeneity of blood flow to white muscle. The spatial heterogeneity of flow to muscle prevented accurate estimation of total flow to this tissue based on the microsphere deposition of a few sub-samples. Instead, a novel approach, based on the whole animal counting of the eviscerated carcass was used to measure blood flow to white muscle. The scaling relationships for tissue mass in catfish (63–1873 g) followed the allometric equation (aW^b) and tended to exhibit negative allometry, with organ weight decreasing in proportion to body weight. The b values for most tissues ranged between 0·83 and 1·0. The relative mass of the brain showed the greatest decline and with a b value of 0·32. The results, together with previous data on cardiac output, permitted calculation of organ blood flow rates in channel catfish.

Key words: regional blood flow; microspheres; allometry; catfish.

INTRODUCTION

Physiologically based pharmacokinetic (PBPK) modelling is gaining acceptance rapidly as a valuable approach for predicting the accumulation and tissue distribution of xenobiotics in fish (Nichols *et al.*, 1990, 1991; Law *et al.*, 1991; Abbas & Hayton, 1997). These models incorporate specific physiological parameters which can be adjusted to allow estimation of chemical exposures and tissue dosimetry among multiple fish species of different body sizes and/or during changing environmental conditions. However, a current limitation to the application of PBPK models is the lack of species-specific, physiological information needed to construct these models for a broad range of fish species. Perhaps the most important set of physiological parameters utilized by these models are tissue blood flow rates. Unfortunately, these parameters have been described for only a few fish species such as rainbow trout *Oncorhynchus mykiss* (Walbaum), albacore tuna *Thunnus alalunga* Bonnaterre and largescale sucker

¶Author to whom correspondence should be addressed. Tel.: 509 376 5031; fax: 509 376 9449; email: ir_schultz@pnl.gov

0022–1112/99/061275+12 $30.00/0

Catostomus macrocheilus Girard (Barron *et al.*, 1987; White *et al.*, 1988; Kolok *et al.*, 1993). Although blood flows can be directly measured in specific vessels using indwelling flow probes, the more common approach to determining tissue perfusion is to measure the relative distribution of cardiac output to specific tissues using synthetic microspheres. When microspheres are injected carefully into the blood stream they become entrapped in capillary beds in direct proportion to the total blood flow to each tissue. In fishes such as salmonids, this can be accomplished by direct injection into the dorsal aorta (Barron *et al.*, 1987), while in other species, the microspheres must be injected into a branchial artery to ensure all microspheres enter the arterial bloodstream prior to initial arterial branching (Kolok *et al.*, 1993).

Channel catfish *Ictalurus punctatus* Rafinesque are an important aquacultural and research test organism and have become the primary warm water fish species used in toxicological and pharmacological studies in fish. Previous researchers have described respiratory and cardiovascular aspects of catfish physiology (Burggren & Cameron, 1980; McKim *et al.*, 1994) and PBPK models for channel catfish have been described recently (Nichols *et al.*, 1993, 1996). However, the relative blood distribution in channel catfish has not been measured and PBPK models developed for channel catfish have relied on blood flow distribution data obtained from rainbow trout. In this study, we injected channel catfish with radiolabelled microspheres via a branchial artery or the dorsal aorta. The amount of radioactivity in tissues was used to quantify the number of entrapped microspheres and calculate blood flow distribution. These experiments were performed at 21° C using channel catfish weighing between 727 and 1050 g. These experimental conditions are analogous to those used by McKim *et al.* (1994) who measured the cardiac output ($\dot{Q}$) of channel catfish. In the second part of the present study we determined the wet weight of selected tissues from a total of 46 male and female channel catfish ranging in weight from 63 to 1873 g and determined the allometric relationships for tissue weight and body mass. These data have applications in body size scaling of physiological processes and were used to aid in calculating tissue perfusion rates in different-sized (5 and 870 g) channel catfish.

MATERIALS AND METHODS

Catfish used for definitive blood flow distribution experiments (870 ± 144 g mean ± S.D. $n=6$) were field collected near the Savannah River Ecology Laboratory, Aiken, SC, U.S.A. Additional catfish used in pilot experiments and allometry determinations were obtained from commercial suppliers (Orangeburg Aquaculture Cordova, SC, U.S.A. and Fenders Fish Hatchery, Baltic, OH, U.S.A.). Immediately upon arrival at the laboratory, all fish received a 2 h prophylactic treatment in a 0·25-mg l^{-1} solution of malachite green (Sigma Chemical, St Louis, MO, U.S.A.). Catfish were held in 600-l, re-circulating water, fibreglass aquaria (LS 900, Frigid Units, Toledo, OH, U.S.A.) containing reconstituted hard water (USEPA 1980) and 1% (w/v) NaCl. All fish were maintained at 21° C for a minimum of 2 weeks prior to use in experiments. The loading density of fish in all aquaria was maintained below 5 g l^{-1}. Half of the aquarium water was replaced biweekly. Chemical characteristics of the freshly prepared water were: total alkalinity 110–120 mg l^{-1} (as $CaCO_3$), hardness 160–180 mg l^{-1} (as $CaCO_3$), and pH 7·9. Temperature and pH were monitored daily, and ranged from 20 to 22° C and 7·7 to 7·9, respectively. Catfish were fed a maintenance ration of 2% of their body mass three

times per week with soft, moist pelleted feed (Rangen Inc., Buhl, ID, U.S.A.), but were fasted for 48 h before microsphere injection.

SURGICAL PROCEDURES

Preliminary studies for microsphere injection utilized catfish fitted with a dorsal aortic cannula that was inserted as described previously (Schultz *et al.*, 1996; Schultz & Newman, 1997). Definitive experiments used six catfish fitted with an efferent branchial artery cannula, inserted occlusively into the second gill arch using 28-G Teflon tubing (Zeus Inc., Raritan, NJ, U.S.A.) and a modification of procedures described previously for the sea raven *Hemitripterus americanus* Pallas and largescale sucker (Farrell, 1986; Kolok *et al.*, 1993). Briefly, catfish were anaesthetized using 150-mg l^{-1} MS-222 and placed laterally in a foam lined, plexiglas brace. One side of the gills was irrigated continuously with oxygenated water containing MS-222. The second gill arch on the opposite side was isolated by anchoring the operculum in an open position using a small suture tied to a nearby support. Two sutures, spaced 0·5 cm apart, were placed at the ventral base of the gill arch to block the afferent flow permanently. Next, two sutures (1–2 cm apart) were placed near the dorsal attachment of the gill arch and tied loosely to obstruct flow through the efferent branchial artery temporarily. A 1-cm portion of gill filaments was trimmed from the arch and a V-shaped incision made to expose the branchial arteries. The Teflon cannula was inserted 2–3 cm into the efferent branchial artery, past the loosened sutures. The sutures were then secured permanently and the trailing portion of the cannula tied to the ventral portion of the arch using two additional sutures. The cannula was allowed to exit from the base of the operculum and secured to the ventral surface of the catfish with two sutures spaced 10 cm apart. A final suture was placed near the posterior portion of the dorsal fin, positioning the cannula in the central portion of the fish. After surgery, catfish were transferred to floating, polyethylene cages (51 cm diameter) housed in 500-l plastic aquaria. The end of the cannula was attached to a 1-ml syringe which was filled with a modified teleost saline [as described by Houston (1990), except that albumin was not added] which floated above the fish inside the cage. All catfish were allowed 24 h recovery following surgery before flood flow distribution experiments were conducted.

BLOOD FLOW DISTRIBUTION AND MICROSPHERE INJECTION

Radiolabelled microspheres were purchased from New England Nuclear (Wilmington, DE, U.S.A). Microspheres injected via the efferent branchial artery were $15{\cdot}5 \pm 0{\cdot}1\,\mu m$ (mean ± S.D.) in diameter and labelled with ^{57}Co. Preliminary experiments used microspheres of diameter $10 \pm 0{\cdot}1\,\mu m$ labelled with ^{153}Gd and were injected into the dorsal aorta. Microspheres were injected as a suspension in 0·9% (w/v) NaCl and 0·01% (v/v) Tween 80. The volume of fluid injected into each fish ranged between 0·4 and 0·6 ml kg^{-1} and contained 4×10^6 spheres kg^{-1} (82 μCi kg^{-1}). Prior to injection, the microsphere mixture was vortexed for 1 min, then placed in an ultra-sonicator (Fisher Scientific model FS14) for 5 min. A 0·8-ml aliquot of the mixture was loaded into a 1-ml gas tight syringe which contained a micro stirrer bar (0·16 × 0·8 cm). A small magnetic stirrer was placed near the syringe, which allowed continuous agitation of the microsphere suspension during injection into the fish. This prevented settling and aggregation of the microspheres during injection, and ensured that a homogeneous mixture was injected. After injection, the cannula was flushed with 0·2 ml of saline and a 0·1-ml aliquot of the injectate was removed from the dosing syringe for calculation of the administered dose.

Catfish were killed 15 min after injection by placing each fish into an oxygenated, ice and water bath containing 200-mg l^{-1} MS-222. After 5 min, the catfish was removed from the bath and a 5-ml blood sample was collected from the dorsal aorta using a 5-ml syringe attached to a 23-G needle. Next, all gill arches were removed and the injected gill arch separated from the remaining gill arches. A large skin sample (7–10 g) was removed from the lateral portion of the fish extending between the caudal penduncle and operculum. Skin samples were carefully trimmed of any adjoining muscle. Duplicate red muscle samples (3–5 g) were collected after skin removal from the midline region of the

fish. Three white muscle samples (5–7 g) were removed from anterior, middle and posterior regions of the fish and trimmed to remove any residual skin and red muscle. The remaining tissues were removed as described below.

Radioactivity in tissue samples was determined by counting the samples to a 2σ error of 1% in an automated 7·6-cm wide × 8·3-cm high well-type NaI(Tl) gamma counter (Packard Auto-gamma® model 5530, Packard Instrument Company, Meriden, CT, U.S.A.). The eviscerated catfish (carcass remaining after dissection) was placed in a Marinelli beaker (GA-MA & Associates, Inc., Miami, FL, U.S.A.) and the whole body ^{57}Co activity was measured using a 7·6-cm wide × 7·6-cm high well-type NaI(Tl) solid scintillator detector/photomultiplier and multichannel analyser (Canberra Series 85, Canberra, Meriden, CT, U.S.A.). This ^{57}Co count rate was normalized to the Packard gamma counter by homogenizing the carcass in a Waring blender and determining the ^{57}Co activity in aliquots of this homogenate. This procedure allowed calculation of microsphere recovery based on comparison between the total radioactivity in dissected tissues and carcass, and the injected dose. Prior to measuring the remaining ^{57}Co activity in the carcass, any visible red muscle was removed. The injected dose was calculated from the total ^{57}Co activity injected into the fish minus the residual radioactivity in the cannula and cannulated gill arch (which we assumed to be trapped locally within the arch).

Blood flow distribution to each organ was calculated as a percentage from the ratio of the radioactivity in the whole organ to the injected dose. For red muscle, the relative flow was based on the averaged count rate in two sub-samples (weight normalized) then adjusted for the relative mass (assumed to equal 0·05). This approach was considered misleading for white muscle because of the high spatial heterogeneity of microsphere lodging. Instead, the remaining ^{57}Co activity in the eviscerated carcass was used to determine blood flow distribution to white muscle. The remaining muscle mass in the eviscerated carcass was calculated from the difference between the carcass weight and the mass of the skeleton. Whole body counting was considered a more accurate method of determining the microsphere deposition in white muscle because the sample size approached 80–90% of the total muscle mass. The local density (LD) of microsphere lodging in white muscle was calculated from the ratio of ^{57}Co activity in the three sub-samples to the ^{57}Co activity determined for the carcass (normalized to the mass of each sub-sample and adjusted mass of the carcass).

The tissue blood flow rate ($\dot{V}_b$; ml h^{-1} g^{-1} tissue) was calculated from the fraction of the microsphere dose lodged within a gram of tissue and the resting cardiac output ($\dot{Q}$) for channel catfish:

$$\dot{V}_b = \dot{Q}\ (\text{ml h}^{-1}\ \text{kg}^{-1}) \times W \times Q_t \qquad (1)$$

where $\dot{Q}$ was assumed to equal 2400 ml h^{-1} kg^{-1} as determined in channel catfish by McKim *et al.* (1994), W = fish weight (kg) and Q_t = fraction of $\dot{Q}$ per g of tissue (blood flow distribution ÷ tissue mass).

RELATIVE TISSUE MASS

Tissue masses were measured from 23 male and female channel catfish (including catfish used in the blood flow distribution studies) ranging in body weight from 63 to 1873 g. All catfish were fasted for 24–48 h and were killed by immersion in an MS-222 ice and water bath as described above. Visceral organs (stomach/oesophagus, intestines, liver, head kidney, spleen, trunk kidney and swim bladder) and brain were removed completely and the wet weight was recorded. Abdominal fat was removed when present. The total skin mass was estimated in three separate individuals (body weight 511–515 g) by the complete removal of all adjoining skin from the carcass (excluding the fins). The mass of white muscle was estimated in these individuals by dissecting all visible red muscle from the carcass and then allowing dermestid beetles *Dermestes vulpinus* Kalik to consume the remaining muscle. The white muscle mass was calculated from the change in carcass weight after complete muscle removal by the dermestid beetles. The mass of the skeleton (remaining portion of carcass) was also recorded at this time. Red muscle

was considered to be 5% of the total muscle mass, based on the dissection of red muscle from these fish and is in the range of values described for other teleosts (Gill *et al.*, 1989).

RESULTS

METHODOLOGY

Initial experiments using 10-μm microspheres administered via the dorsal aorta, indicated that microsphere distribution to the head kidney was not measured accurately because the cannula could not be positioned anterior to the arterial branch to this organ. In addition, there was always unacceptably high activity in the gills (>5% of the dose) which indicated poor lodging of the 10-μm microspheres. In contrast, the 15·5-μm microspheres administered via the efferent branchial artery provided excellent lodging with <5% of the injected radioactivity accumulating in the blood and gill filaments opposite to the side injected. The recovery of microspheres from each of the dissected organs and the carcass was consistently high (81–101%) and no unexplained loss of microspheres was observed.

MICROSPHERE DISTRIBUTION AND RELATIVE TISSUE MASS

The results of microsphere distribution experiments using the 15·5-μm microspheres indicated the majority of the microspheres distributed to the head kidney, trunk kidney, white and red muscle, skin and the swim bladder (Table I). There was only minimal microsphere distribution to the liver, with most individuals having less than 0·1% entrapment of the injected dose. A notable exception was a single fish which had >12·45% of the microsphere dose in the liver (Table I). This same fish also had the highest entrapment of microspheres in the stomach and intestines. In general, the distribution of microspheres to visceral organs was characterized by a high degree of between-animal variation with the range of values observed often exceeding 10-fold for specific organs. The main exception was the trunk kidney where most values were within a factor of 2. Although mean values for the distribution of microspheres is reported for each tissue in Table I, it should be recognized that relative blood flow distribution in catfish exhibited a high degree of variation. This observed variation in microsphere distribution suggests substantial plasticity in the organ-specific tissue perfusion of resting channel catfish.

The majority of administered microspheres remained in the eviscerated carcass, which consisted of muscle, bone and cartilage. We have assumed there was negligible entrapment of microspheres in bone and cartilage and considered that the remaining microspheres were lodged in the non-dissected portions of muscle. When the weight-normalized entrapment of microspheres in the three sub-samples of white muscle is compared to the value determined for the carcass, it was evident that substantial spatial heterogeneity of microsphere entrapment occurred. The range in local densities of microspheres frequently varied up to a factor of 10 and in one instance varied 50-fold (Table I). The heterogeneity did not appear to correlate with specific regions of muscle, as the level of entrapment among samples of posterior, mid and anterior portions of muscle appeared to be random among individuals (data not shown). Because of the high degree of heterogeneity among the three sub-samples of muscle removed, the estimation of

TABLE I. The distribution of ^{57}Co-labelled microspheres in six channel catfish after injection *via* the second efferent branchial artery

Tissue	Distribution of blood flow to whole tissues (% of injected microspheres)						Mean ± S.D.	Tissue mass* (% *W*)
Head kidney	17·6	0·74	5·81	2·14	6·90	1·00	5·70 ± 6·4	0·23 ± 0·07
Trunk kidney	0·47	5·41	5·66	2·96	2·25	2·00	3·12 ± 2·0	0·46 ± 0·17
Liver	0·02	0·04	0·62	0·08	12·45	0·02	2·2 ± 5·0	1·09 ± 0·33
Stomach	0·22	0·03	0·21	0·043	0·98	0·011	0·25 ± 0·36	1·09 ± 0·18
Intestines	0·03	0·05	0·04	0·06	0·64	0·0086	0·14 ± 0·25	0·99 ± 0·3
Pyloric caeca	—	0·006	0·001	0·02	0·27	—	0·07 ± 0·13	0·67 ± 0·02
Testes	0·011	—	0·05	0·02	—	—	0·03 ± 0·02	0·16 ± 0·08
Ovaries	—	0·12	—	—	0·065	1·62	0·60 ± 0·88	0·94 ± 0·33
Swim bladder	—	4·85	0·14	1·39	0·032	0·74	1·43 ± 1·9	0·45 ± 0·07
Brain	0·12	0·46	0·32	0·01	0·07	0·07	0·18 ± 0·17	0·06 ± 0·01
Fat	0·016	0·001	0·008	0·01	0·006	—	0·01 ± 0·005	—
Skin	1·74	0·43	2·37	0·70	0·167	1·05	1·08 ± 0·8	4·70 ± 0·2
Spleen	—	0·006	0·0032	0·007	0·001	0·002	0·004 ± 0·003	0·91 ± 0·26
Skeleton								17·7 ± 0·6
Red muscle	1·64	2·83	20·6	2·98	3·83	0·92	5·46 ± 7·5	5
White muscle†	77·0	74·0	47·0	71·0	73·0	91·0	72·2 ± 14·3	45·0 ± 1·2
LD‡	0·02–1·0	0·3–3·6	1·0–8·2	0·3–0·4	0·02–0·2	0·1–0·25		
Recovery (%)§	98·8	91·9	82·8	81·4	100·6	98·4	96·2 ± 7·7	
BW (gm)	800	730	727	1032	884	1050	870 ± 144	

*All tissues were removed in their entirety except fat, red and white muscle. See text for methods used to determine white and red muscle relative mass.

†These values were determined from measurements of the remaining radioactivity in the skinned and eviscerated carcass.

‡LD is the regional, local density of microspheres in selected pieces of white muscle. These values represent the ratio of the mass specific microsphere deposition amongst sub-samples of white muscle relative to the deposition in the carcass (normalized to the total mass of muscle). A value of 1·0 means the sub-sample contained the fractional equivalent of microspheres compared to the carcass while a value of 0·1 means the sub-sample contained 1/10 the amount.

§Recovery was determined by the total activity in tissue samples + the activity in the eviscerated carcass divided by the dose.

was considered to be 5% of the total muscle mass, based on the dissection of red muscle from these fish and is in the range of values described for other teleosts (Gill *et al.*, 1989).

RESULTS

METHODOLOGY

Initial experiments using 10-μm microspheres administered via the dorsal aorta, indicated that microsphere distribution to the head kidney was not measured accurately because the cannula could not be positioned anterior to the arterial branch to this organ. In addition, there was always unacceptably high activity in the gills (>5% of the dose) which indicated poor lodging of the 10-μm microspheres. In contrast, the 15·5-μm microspheres administered via the efferent branchial artery provided excellent lodging with <5% of the injected radioactivity accumulating in the blood and gill filaments opposite to the side injected. The recovery of microspheres from each of the dissected organs and the carcass was consistently high (81–101%) and no unexplained loss of microspheres was observed.

MICROSPHERE DISTRIBUTION AND RELATIVE TISSUE MASS

The results of microsphere distribution experiments using the 15·5-μm microspheres indicated the majority of the microspheres distributed to the head kidney, trunk kidney, white and red muscle, skin and the swim bladder (Table I). There was only minimal microsphere distribution to the liver, with most individuals having less than 0·1% entrapment of the injected dose. A notable exception was a single fish which had >12·45% of the microsphere dose in the liver (Table I). This same fish also had the highest entrapment of microspheres in the stomach and intestines. In general, the distribution of microspheres to visceral organs was characterized by a high degree of between-animal variation with the range of values observed often exceeding 10-fold for specific organs. The main exception was the trunk kidney where most values were within a factor of 2. Although mean values for the distribution of microspheres is reported for each tissue in Table I, it should be recognized that relative blood flow distribution in catfish exhibited a high degree of variation. This observed variation in microsphere distribution suggests substantial plasticity in the organ-specific tissue perfusion of resting channel catfish.

The majority of administered microspheres remained in the eviscerated carcass, which consisted of muscle, bone and cartilage. We have assumed there was negligible entrapment of microspheres in bone and cartilage and considered that the remaining microspheres were lodged in the non-dissected portions of muscle. When the weight-normalized entrapment of microspheres in the three sub-samples of white muscle is compared to the value determined for the carcass, it was evident that substantial spatial heterogeneity of microsphere entrapment occurred. The range in local densities of microspheres frequently varied up to a factor of 10 and in one instance varied 50-fold (Table I). The heterogeneity did not appear to correlate with specific regions of muscle, as the level of entrapment among samples of posterior, mid and anterior portions of muscle appeared to be random among individuals (data not shown). Because of the high degree of heterogeneity among the three sub-samples of muscle removed, the estimation of

TABLE II. Allometric relationship of tissue wet weight to body weight in channel catfish

Tissue	Tissue allometry		MSE	r^2
	a	b		
Head kidney	0·0026 ± 0·002	0·96	0·09	0·90
Liver	0·0161 ± 0·002	0·95	0·07	0·88
Stomach	0·004 ± 0·002	1·16	0·06	0·96
Intestines	0·014 ± 0·001	0·81	0·07	0·83
Swim bladder	0·004 ± 0·001	1·02	0·06	0·95
Trunk kidney	0·007 ± 0·004	0·87	0·07	0·86
Brain	0·064 ± 0·011	0·32	0·03	0·76
Spleen	0·0002 ± 0·0002	1·2	0·1	0·88
Heart	0·002 ± 0·001	0·81	0·05	0·91

Values were obtained from a plot of log tissue wt. (g) *v.* log body wt (g).

the total distribution of microspheres to white muscle was based on the value determined from the eviscerated carcass.

The wet weight of most organs declined in direct proportion to increasing body size and a cursory examination of the data indicated no gender specific trends (Table II and Fig. 1). Brain mass exhibited the greatest decrease in relative size with increasing body weight (Table II). The body size scaling relationships for all tissues examined appeared to follow the allometric equation ($y=aW^b$) (Fig. 1) and r^2 values for most tissues exceeded 0·9 (Table II).

DISCUSSION

The results of this study are consistent with previous blood flow distribution studies that have concluded that the majority of $\dot{Q}$ in freshwater fish is distributed to muscle and the kidneys (Barron *et al.*, 1987; reviewed in Bushnell *et al.*, 1992; Kolok *et al.*, 1993; Butler & Ouidit, 1994). Remaining tissues generally received <1% of $\dot{Q}$ with the exception of the skin and swim bladder, which received between 1·08% and 1·43%. There was only minimal entrapment of microspheres in the liver, and estimates of arterial blood flow to this organ are lower than previously reported for rainbow trout (Barron *et al.*, 1987) and American eel *Anguilla rostrata* Lesueur (Butler & Ouidit, 1994) but similar to the flow (~1% of $\dot{Q}$) in the largescale sucker (Kolok *et al.*, 1993). A substantial portion of the blood flow to the liver can be delivered by the hepatic portal vein (McLean & Ash, 1989) which is not measured by the microsphere technique. This may have caused the total flow to the liver to be underestimated in the present study. However, the fraction of $\dot{Q}$ delivered to the gastrointestinal system (stomach, intestines and pyloric caeca) which contributes to the portal system flow, was also very low. The combined microsphere distribution to the gastrointestinal tract and liver was still <1% for all but one catfish. This suggests that in fasted, benthic freshwater fish such as the channel catfish and largescale sucker, blood flow to the liver is at a minimal level (i.e. <1% of $\dot{Q}$). In other fish species, it has been demonstrated that gastrointestinal blood flow can increase up

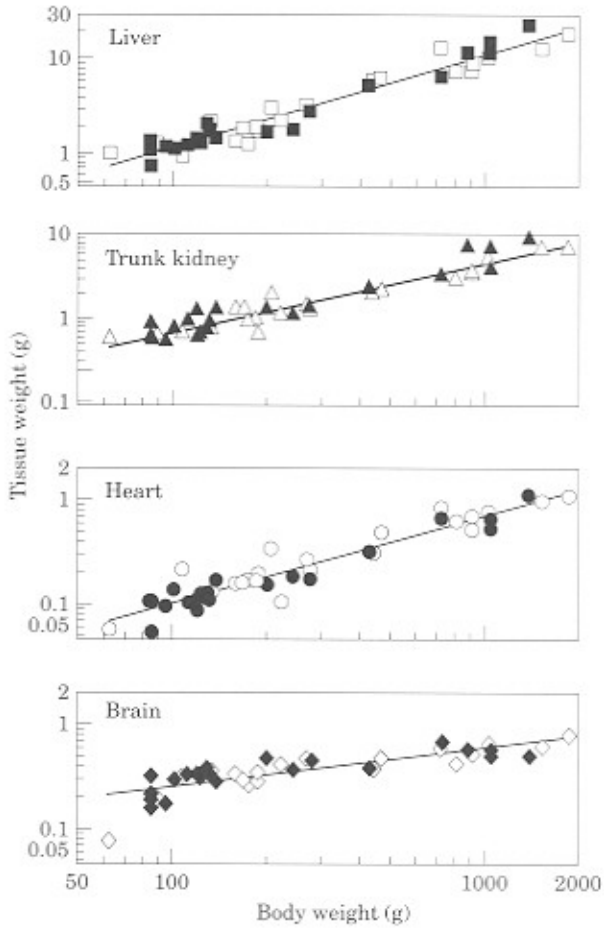

FIG. 1. Allometric scaling of selected tissue wet weights to total fish weight (W) in male (solid symbols) and female (open symbols) channel catfish. The coefficients describing the allometric equation (aW^b) for each tissue are shown in Table II.

to 70–100% of fasted values following feeding (Axelsson *et al.*, 1989; Axelsson & Fritsche, 1991). Although all catfish used in the present study had been fasted for 48 h by the time of microsphere injection, between-animal variation in liver and gastrointestinal flow may have been due in part, to differences in food consumption prior to surgery. An additional source of error may result from incomplete mixing of the microspheres in the blood during the injection process. However, this would appear unlikely as extensive precautions were taken to prevent clumping of the microspheres and the small fraction of injected microspheres entrapped in the gills is an indication that adequate mixing occurred.

The large fraction of microspheres remaining in the carcass (determined from whole body counting) demonstrated that most (47–91%) was present in the white muscle. The large spatial heterogeneity of microsphere entrapment (determined from tissue sub-samples) in white muscle indicated extensive variation (10–50-fold, see LD values Table I), in blood flow to this tissue. The prevalence of blood

McLean, E. & Ash, R. (1989). Chronic cannulation of the hepatic portal vein in rainbow trout, *Salmo gairdneri*: a prerequisite to net absorption studies. *Aquaculture* **78,** 195–205.

Myagkov, N. A. (1991). The brain sizes of living elasmobranchii as their organizational level indicator. I. General analysis. *Journal für Hirnforschung* **32,** 553–561.

Nichols, J. W., McKim, J. M., Andersen, M. E., Gargas, M. L., Clewell III, H. J. & Erickson, R. J. (1990). A physiologically based toxicokinetic model for the uptake and disposition of waterborne organic chemicals in fish. *Toxicology and Applied Pharmacology* **106,** 433–447.

Nichols, J. W., McKim, J.M., Lien, G. J., Hoffman, A. D. & Bertelsen, S. L. (1991). Physiologically based toxicokinetic modeling of three chlorinated ethanes in rainbow trout (*Onchorhynchus mykiss*). *Toxicology and Applied Pharmacology* **110,** 374–389.

Nichols, J. W., McKim, J. M., Lien, G. J., Hoffman, A. D., Bertelsen, S. L. & Gallinat, C. A. (1993). Physiologically based toxicokinetic modeling of three waterborne chloroethanes in channel catfish, *Ictalurus punctatus*. *Aquatic Toxicology* **27,** 83–112.

Nichols, J. W., McKim, J. M., Lien, G. L., Hoffman, A. D., Bertelsen, S. L. & Elonen, C. M. (1996). A physiologically based toxicokinetic model for dermal absorption of organic chemicals by fish. *Fundamental and Applied Toxicology* **31,** 229–242.

Oikawa, S. & Itazawa, Y. (1984). Allometric relationship between tissue respiration and body mass in the carp. *Comparative Biochemistry and Physiology A* **77,** 415–418.

Oikawa, S. & Itazawa, Y. (1993*a*). Allometric relationship between tissue respiration and body mass in a marine teleost, Porgy *Pagrus major*. *Comparative Biochemistry and Physiology A* **105,** 129–133.

Oikawa, S. & Itazawa, Y. (1993*b*). Tissue respiration, and relative growth of parts of body of a marine teleost, Porgy *Pagrus major*, during early life stages with special reference to the metabolism rate relationship. *Comparative Biochemistry and Physiology A* **105,** 741–744.

Platel, R. & Vesselkin, N. P. (1986). The analysis of the brain-body allometries in adults of *Lamptera fluviatilis*. *Cybium* **10,** 143–153.

Schmidt-Nielsen, K. (1984). *Scaling: Why Is Animal Size So Important*. Cambridge: Cambridge University Press.

Schultz, I. R. & Newman, M. C. (1997). Interspecies differences in the toxicokinetics of methyl mercury in fish. *Environmental Toxicology and Chemistry* **16,** 990–996.

Schultz, I. R. & Hayton, W. L. (1999). Interspecies scaling of the bioaccumulation of lipophilic xenobiotics in fish: an example using trifluralin. *Environmental Toxicology and Chemistry* (in press).

Schultz, I. R., Peters, E. L. & Newman, M. C. (1996). Toxicokinetics and disposition of inorganic mercury and cadmium in channel catfish after intravascular administration. *Toxicology and Applied Pharmacology* **140,** 39–50.

Tort, L., Flos, R. & Balasch, J. (1984). Factors influencing tissue oxygen consumption in dogfish. *Comparative Physiology and Ecology* **9,** 201–206.

USEPA (1980). *Quality Assurance Guidelines for Biological Testing*. EPA-600/4-78-043. Environmenal Monitoring Series. Cincinnati, OH: US Environmental Protection Agency. Environmental Monitoring and Support Laboratory.

Weatherley, A. H. (1990). Approaches to understanding fish growth. *Transactions of the American Fisheries Society* **119,** 662–672.

Weatherley, A. H. & Gill, H. S. (1987). *The Biology of Fish Growth*. London: Academic Press.

White, F. C., Kelly, R., Kemper, S., Schumaker, P. T., Gallagher, K. R. & Laurs, R. M. (1988). Organ blood flow haemodynamics and metabolism of the albacore tuna, *Thunnus alaunga* (Bonnaterre). *Experimental Biology* **47,** 161–169.

TABLE III. Tissue perfusion calculated for selected tissues in large (870 g) and small (5 g) catfish

Tissue	V_b (ml h^{-1} g-tissue^{-1})*	
	870 g	5 g
Head kidney	57·4	196·0
Liver	3·92	13·5
Stomach	0·25	2·61
Intestines	0·36	1·39
Swim bladder	1·43	30·2
Trunk kidney	11·1	49·3
White muscle†	2·45	—
Red muscle	3·36	—
Skin	1·08	—
Fat	0·02	—

*Values for the 870 g catfish are based on data shown in Table I and $\dot{Q}$=2400 ml h^{-1} kg^{-1} as reported by Mckim *et al.* (1994). Values calculated for a 5-g catfish were made assuming blood distribution follows the allometric relationship for tissue weight shown in Table II and $\dot{Q}$ scales to a body weight exponent value of 0·75 ($\dot{Q}$=8500 ml h^{-1} kg^{-1}).

rates of selected visceral tissues in a 5-g catfish, shown in Table III. When compared with values calculated for larger catfish, the perfusion of visceral tissues is predicted to increase from four- to 16-fold across a body size range of 174-fold (5–870 g). This substantial change in tissue perfusion rates with body size illustrates the need to consider allometric influences when comparing blood flow rates among fishes.

CONCLUSION

The continued development of more sophisticated PBPK models for use in ecological and environmental risk assessments has allowed the greater incorporation of fish physiological data to help predict the tissue distribution of xenobiotics in fish. To allow further development and use of these models, an improved understanding of tissue blood flow rates and factors which can affect blood flow is needed. Previous studies have measured the effects of acclimation temperature, feeding and exercise on blood flow (Barron *et al.*, 1987; Axelsson & Fritsche, 1991; Kolok *et al.*, 1993). Another important variable that needs to be addressed is the influence of body size on blood flow rates. The direct measurement of blood flow in smaller individuals is impractical and can be estimated only by indirect methods. The limited experimental data suggest that relative distribution of blood (percentage of $\dot{Q}$) to visceral tissues increases with decreasing body size. This conclusion is based on the allometric relationships presented in this and other studies for the relative size of visceral organs and additional reports that mass specific, tissue oxygen demands of visceral organs are higher in juvenile fish (Tort *et al.*, 1984; Oikawa & Itazawa, 1984, 1993*b*).

flow heterogeneity in fish is unknown as most blood flow studies have used averaged values calculated from a few muscle sub-samples. Blood flow heterogeneity has been well characterized for skeletal and cardiac muscle in mammals (King *et al.*, 1985; Basingthwaighte *et al.*, 1987; reviewed in Duling *et al.*, 1987). In these studies, large numbers of tissue sub-samples are removed (up to 200) to allow characterization of a probability density function to describe regional blood flow to muscle (Bassingthwaighte *et al.*, 1987). Spatial heterogeneity of blood flow to cardiac muscle can be constant over time; for example, specific regions of muscle consistently receive substantially more or less blood flow than the average value (King *et al.*, 1985). The observed range in local densities of microsphere deposition in catfish white muscle was consistent with the spatial heterogeneity observed in muscle from mammalian species (Duling *et al.*, 1987). Future blood flow studies in fish should incorporate whole tissue measurements of white muscle and/or the removal of larger numbers of muscle sub-samples to characterize the relative flow to white muscle better.

Previous studies of the body size scaling of fish tissues have shown that visceral tissue mass decreases in proportion with increasing body weight (negative allometry: Weatherley & Gill, 1987; Weatherley, 1990). Consequently, as body size increases, the relative proportion of muscle also increases (positive allometry) at the expense of the relative mass of visceral tissues. Our results for channel catfish are consistent with these observations as the relative weight of most visceral organs declined in proportion to body weight (Table II). This was most apparent for the brain, which exhibited the greatest degree of negative allometry with a b value of 0·32 (Table II). There are a few reports of allometric relationships for brain size in other fishes, with reported b values ranging from 0·41 to 0·61 in diverse fish groups such as lampreys, elasmobranchs and teleosts (Bauchot *et al.*, 1979; Platel & Vesselkin, 1986; Myagkov, 1991; Oikawa *et al.*, 1993*a*). A commonality of these studies is that lower b values are observed when comparing the scaling relationships among postjuvenile specimens. Thus, a large decrease in the relative mass of the brain with increasing body size appears to be a characteristic of adult fishes. This was especially true for channel catfish, where it appeared that brain size approached a near maximal value at a body weight range of 200–500 g, beyond which only marginal increases in brain size occurred (Fig. 1).

The tissue perfusion rates calculated for the 870-g catfish using equation (1) and the previously published value of $\dot{Q}$ in catfish, 2400 ml h^{-1} kg^{-1} (McKim *et al.*, 1994), are summarized in Table III. In order to estimate tissue perfusion rates in small catfish (arbitrarily defined as 5 g body mass), the relative blood flow (Q_t) and $\dot{Q}$ need to be scaled from values measured in larger catfish. To accomplish this, Q_t was adjusted for a 5-g channel catfish (Q_{t5}) using the change in relative tissue mass (M) between a 5- and 870-g catfish, i.e. $Q_{t5}=Q_{t870} \times M_5 \times M^{-1}{}_{870}$. The relative mass of tissues for a 5-g channel catfish was calculated using the allometric relationships shown in Table II. The allometry of $\dot{Q}$ has not been established in fish (Farrell & Jones, 1992). Therefore, we assumed $\dot{Q}$ scales to a body weight exponent of 0·75, which is consistent with values reported for mammals (Schmidt-Nielsen, 1984). Based on this assumption, the calculated $\dot{Q}$ for a 5-g catfish was estimated to be 8500 ml h^{-1} kg^{-1}. This value was used in the calculations for the perfusion